

Single Cell Trapping by Superhydrophobic/Superhydrophilic Microarrays

Paavo Raittinen, Pinja Elomaa, Päivi Saavalainen, and Ville Jokinen*

Single cell trapping is demonstrated on superhydrophobic–superhydrophilic patterned microarrays. Superhydrophilic spots that are twice the size of the cells to be trapped are found to be optimal for obtaining single cell trapping. The single cell trapping is based on size exclusivity instead of heavy dilution of the cell suspension and relying on Poisson statistics. The superhydrophobic areas of the array are found to be very resistant toward unwanted adhesion of the cells and thus cleaning steps are not needed after deposition. Based on these properties, 20 μm superhydrophilic spots are utilized for trapping two types of immune cells, primary peripheral blood mononuclear cells (PBMCs) and THP-1 cells. The cells are trapped from a 10 μl cell suspension droplet dragged across the surface with different velocities. Single cell trapping efficiencies in the range of 10–30% are shown based on the cell type, the spot type, the seeding velocity and the cell suspension concentration.

between the solid substrate and water. The resulting surface is a composite air/solid surface described by the Cassie–Baxter model^[2] and it is the high air fraction that is responsible for the low adhesion of water. Similar repellency can also be achieved for other liquids. Oil repellency (oleophobicity) requires re-entrant topographies^[3] while repellency of all liquids including extremely low surface tension liquids (omniphobicity), such as fluorinated solvents, utilizes doubly re-entrant geometries.^[4,5] Two promising developments toward potential applications are superhydrophobic/superhydrophilic (SHB/SHL) micropatterns and bio-repellent superhydrophobic surfaces. SHB/SHL patterned surfaces^[6] can be used to control the shapes of droplet and to create

1. Introduction

Superhydrophobic surfaces repel water which causes water droplets to bead up and roll off with very low adhesion and friction. Superhydrophobicity is usually based on a combination of rough topography and a hydrophobic surface chemistry,^[1] which together trap a layer of gas (called the plastron)

droplet arrays with high resolution (in the micrometer range). They have been proposed for many applications,^[7] including cell cultivation,^[8] liquid–liquid extraction^[9] and particle depositions.^[10] Bio-repellency of SHB surfaces is an emerging field and it has been shown that cells typically cannot easily penetrate through the plastron to reach the surface.^[11] Some SHB surfaces can repel blood^[12,13] and kill bacteria,^[14] although the biofouling resistance can be short-lived.^[15]

The cell anti-adhesive properties of SHB surfaces can be utilized for creating cell microarrays. Ishizaki et al.^[16] showed that 3T3 cells cultivated on top of SHB/SHL patterned surfaces preferentially adhered and grew on top of the SHL areas by a ratio of over 10:1. Piret et al.^[17] cultured CHO-K1 on SHB/SHL patterned silicon nanowire arrays. The cells almost exclusively grew on top of the 50 μm sized SHL spots instead of the SHB background. On a non-patterned SHB silicon nanowire surface, no cells were detected on the surface after 48 hours a single washing step.

Single cell trapping for single cell analysis is an application area that seems very promising for SHB/SHL arrays. Single cell biology is expected to be a major step forward from the current cell population average methods^[18] which are currently widely used in biomedical science. Macosko et al.^[19] showed single cell RNA sequencing utilizing droplet microfluidics, where discrete water droplets in oil are created inside a microfluidic channel. With proper dilution, Poisson statistics ensure that some of the droplets only contain a single cell. A competing approach is to utilize microwell arrays. Gierahn et al.^[20] utilized 50–100 μm diameter microwell arrays to trap single cells and barcoding microbeads for RNA sequencing. The array sizes were matched to the size of microbeads and trapping efficiency of 94% for beads was obtained with only 5% of wells without a bead and only

P. Raittinen

Aalto University School of Science
Department of Mathematics and Systems Analysis
Espoo 02150, Finland

P. Elomaa, Dr. P. Saavalainen

University of Helsinki

Faculty of Medicine

Research Program Unit

Translational Immunology Research Program and Department

of Medical and Clinical Genetics

Haartmaninkatu 8, Helsinki 00290, Finland

Dr. V. Jokinen


Aalto University

School of Chemical Engineering

Department of Chemistry and Materials Science

Tietotie 3, Espoo 02150, Finland

E-mail: ville.p.jokinen@aalto.fi

 The ORCID identification number(s) for the author(s) of this article can be found under <https://doi.org/10.1002/admi.202100147>.

© 2021 The Authors. Advanced Materials Interfaces published by Wiley-VCH GmbH. This is an open access article under the terms of the Creative Commons Attribution-NonCommercial License, which permits use, distribution and reproduction in any medium, provided the original work is properly cited and is not used for commercial purposes.

DOI: 10.1002/admi.202100147

approximately 0.5% containing multiple beads. The cells were loaded in smaller quantity to ensure only one cell falls into one well; 80% capture efficiency was obtained with this cell-loading method with a low duplet rate. Microwell arrays preserve the spatial alignment of cells, but sedimentation and the functionalization and washing steps required for the protocols increases the time and complexity of the process. Du et al.^[21] showed a simpler microwell array protocol consisting of smearing the array with a cell suspension followed by smearing with oil to wash and seal in the same step. They showed trapping of *Staphylococcus aureus* ($\approx 1 \mu\text{m}$) with microwells sized $10 \mu\text{m}$ and larger and the distribution followed closely the Poisson distribution. Microarray method using a stencil was used for single cell mass spectrometry by Xie et al.^[22] They utilized a polydimethylsiloxane stencil with $30\text{--}50 \mu\text{m}$ sized holes to pattern cells on ITO coated glass and subsequently analyzed the lipid content of the cells by matrix assisted laser desorption ionization mass spectrometry. With a $40 \mu\text{m}$ spot size, about a quarter of the spots contained a single cell, with equally many or more containing two or three cells.

SHB/SHL arrays have been used for single cell analysis in few previous publications. The group of Levkin has developed SHB/SHL arrays for trapping and cultivating cell populations, including single cells.^[23] They used a methacrylate copolymer based SHB/SHL patterned surface to capture HeLa cells on hydrophilic spot sizes ranging from 350 to $1000 \mu\text{m}$. Up to 19.4% of the spots initially contained a single cell, while some spots had multiple cells. The single cell trapping was obtained by dilution since the spots were much larger than the cells. The cells cultivated on the spots showed good viability. Li et al.^[24] utilized superhydrophobic porous silicon samples patterned with $100 \mu\text{m}$ superhydrophilic spots to capture single human breast cancer cells. Deposition of single cells into four consecutive spots in a row was shown, but statistics of the deposition were not discussed. In these works, the deposition was done either by a sliding droplet^[23] or by droplet dragging^[24] where the superhydrophobic areas remain dry due to the plastron and thus presumably also free of cells. However, due to the size of the spots ($>100 \mu\text{m}$) compared to the size of the cells, the cell trapping was likely based on dilution and Poisson statistics and not size selectivity.

Here we show SHB/SHL microarrays for trapping single immune cells ($\approx 10\text{--}20 \mu\text{m}$) utilizing SHL spots with diameters less than $30 \mu\text{m}$, thus allowing the single cell trapping to be based on size selectivity and not Poisson dilution.

2. Results and Discussion

The single cell trapping concept is shown in **Figure 1a**. A mother droplet (volume $10 \mu\text{l}$) is dragged on top of an SHB array decorated with SHL spots. It leaves behind an array of daughter droplets of roughly five picoliters (estimated from **Figure 1b** using spherical cap assumption) on top of the SHL spots (**Figure 1b**). The SHB surface utilized was fluoropolymer coated black silicon (**Figure 1c**).^[6] The advancing and receding water contact angles of the SHB surface were $167^\circ \pm 1^\circ$ and $167^\circ \pm 1^\circ$, respectively. This surface has been shown to have extremely low adhesion forces with water droplets (nN to μN range).^[25]

The hydrophilic spots were fabricated by utilizing optical lithography. Two types of hydrophilic spots were used: planar silicon spots with hydrophilic chemistry (shown in **Figure 1d**) and nanograss spots with hydrophilic chemistry. The hydrophilic chemistry was plasma cleaned and oxidized silicon, and for both SHL spot types, the contact angles were $<5^\circ$. The diameter d of the hydrophilic spots was varied between $10\text{--}100 \mu\text{m}$. The spots were arranged in a rectangular lattice where the spacing s between the spots was varied between $2d$ and $4d$. Unless otherwise specified, all results are reported with the spot spacing of $2d$. The area density of the spots varied with the size but for the $20 \mu\text{m}$ spot size used for single cell trapping, the area density was roughly $28\,000$ spots per cm^2 .

2.1. Bead Trapping to Optimize Spot Size

To arrive at the correct range of spot sizes leading to effective single cell trapping, a set of preliminary experiments was conducted with polystyrene beads suspensions (**Figures S1 and S2**, Supporting Information). These bead experiments

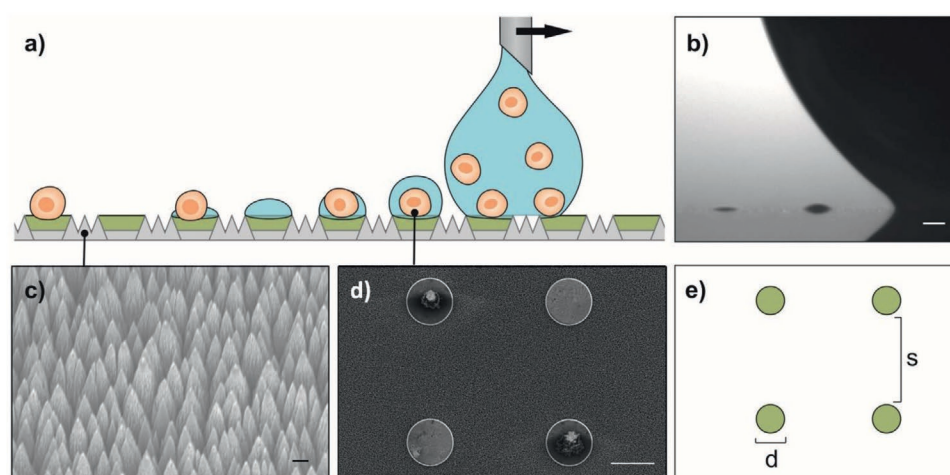


Figure 1. Single cell trapping with superhydrophobic/superhydrophilic patterned surfaces. a) An illustration of the trapping concept. b) Optical micrograph of mother droplet and two daughter droplets (scalebar $100 \mu\text{m}$). c) Scanning electron micrograph of superhydrophobic black silicon nanograss (scalebar $1 \mu\text{m}$). d) Scanning electron micrograph showing single THP-1 cells trapped onto hydrophilic spots. Cells are trapped on top left and bottom right spots (scalebar $20 \mu\text{m}$). e) The geometry of the spot array.

utilized hydrophilic black silicon spots. Polystyrene beads of 10 and 20 μm diameter were chosen since their size and density roughly matches those of cells. The results of the trapping experiments are shown in Figure S1, Supporting Information. For the 20 μm beads, using 40 μm spots resulted in 23.6% of single occupancy and the rest of the spots were empty (Figure S2d, Supporting Information). In contrast, 50 μm spot size with the same 20 μm bead size resulted in 55% singlets, 14% doublets, and no triplets (Figure S2f, Supporting Information). Using 10 μm beads and 20 μm spots, the occupancy rate distribution was 28%, 3.6%, and 0.6%, singlets, doublets, and triplets respectively (Figure S2a, Supporting Information). Moreover, using 10 μm beads with 30 μm spots resulted in significantly larger proportion of doublets and multiples as 40.7% were singlets and roughly 36% doublets or multiples (Figure S2c, Supporting Information). These experiments clearly showed that the optimal spot size is close to two times the size of the beads to be trapped, which is the range we chose for trapping single cells. This rule is sensible for the polystyrene beads, assuming that: the beads can only reside inside the hydrophilic spots, and that the beads are rigid bodies so thus cannot deform due to the forces involved in the process. Spots smaller than twice the diameter of the beads can only fit one bead; however, spots that are too small cannot host any beads. The results also showed that while it would be possible to increase the absolute number of spots with a single bead by simply going above the two to one ratio (in spot diameter versus bead size), this would come at a cost of rapidly increasing percentage of spots containing multiple beads (comparisons between Figure S2a vs Figure S2c, Supporting Information and Figure S2d vs Figure S2f, Supporting Information)

The bead experiments were also utilized to test the effect of the velocity of the mother droplet on the deposition efficiency. The results (Figure S2a, Supporting Information) showed that for 10 μm beads and 20 μm spot size, when deposited at

10 mm min^{-1} velocity, 28.0%, 3.6%, and 0.6% of the spots had one, two, or three beads, respectively (for comparison, Poisson distribution using $\lambda = 0.43$ is 28.0%, 6.0%, and 0.9%, for one, two, three beads per spot, respectively). These results suggest that the bead trapping is dominated by size exclusivity instead of a stochastic process and therefore the spot size can be used to control the single-bead occupancy. Tenfolding the velocity from 10 mm min^{-1} to 100 mm min^{-1} led to significantly reduced number of deposited beads: 9.4%, 1.7%, and 0% of the spots containing one, two, or three beads, respectively (Figure S2b, Supporting Information). This suggests that the seeding velocity can be used to control the deposition efficiency without affecting the underlying occupancy rate distribution (density). It is noteworthy that throughout all performed experiments, no bead deposited on the SHB areas and thus there was no need for any washing steps.

2.2. Single Cell Trapping

Our first single cell trapping test was to compare black silicon (spiked) SHL spots and planar SHL spots. Single cell trapping was tested for primary peripheral blood mononuclear cells (PBMC) extracted from adult human donors. The cells were deposited selectively onto both types of hydrophilic spots, black silicon spots (Figure 2a–c) and planar spots (Figure 2d–f). There was a clear difference between the two spot types: the cells were fully intact when deposited on the planar spots (Figure 2d) but perforated and mechanically lysed by the spikes when deposited on the black silicon spots (Figure 2a). Moreover, using black silicon spots, cells occasionally extended from one spot to another through the hydrophobic regions, forming thin bridge-like channels of cell membrane/debris/DNA between two adjacent spots (Figure 2b). The cell puncture likely

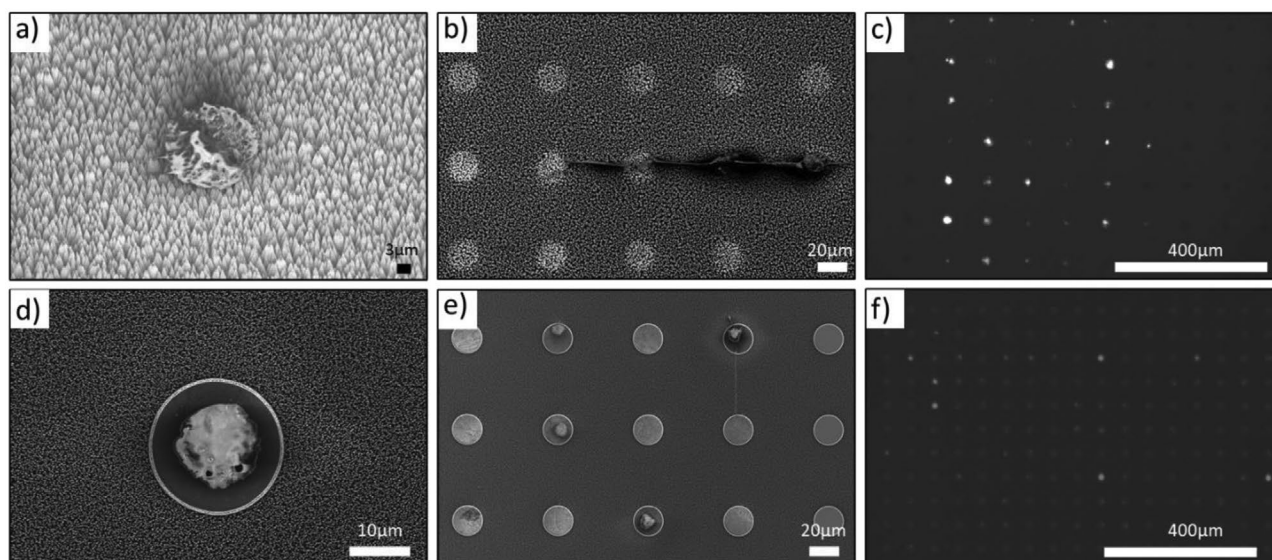


Figure 2. Single cell trapping with SHB/SHL arrays. The hydrophilic spot has in (a–c) a black silicon topography and in (d–f) a planar topography. a,b) Electron micrographs of PBMCs on the black silicon hydrophilic spots. c) Fluorescence stained cell micrographs of PBMCs on the black silicon hydrophilic spots. d,e) Electron micrographs of PBMCs on the planar hydrophilic spots. f) Fluorescence stained cell micrographs PBMCs on the planar hydrophilic spots.

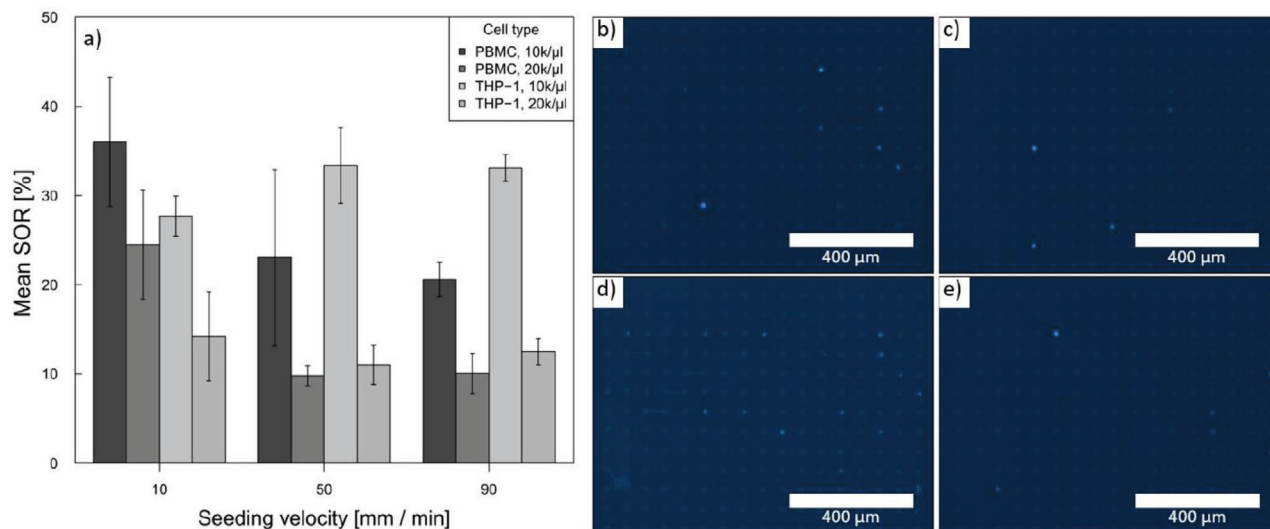


Figure 3. a) Single cell occupancy rate as a function of cell type, seeding velocity, and cell suspension concentration. Fluorescence microscopy images of DAPI stained cells deposited on 20 μm spots: b) PBMC, 10 k μl⁻¹, c) PBMC, 20 k μl⁻¹ d) THP-1, 10k μl⁻¹, e) THP-1, 20 k μl⁻¹.

results from the cells adhering on top of the sharp spikes as the mother droplet moves past the spot. As the cell perforation could be a serious drawback for single-cell analysis applications due to potential cross-contamination in DNA/RNA studies or due to cell death in single cell culturing, we conclude that for single cell trapping applications, planar hydrophilic spots are the better choice. However, the mechanical lysis could also be a benefit for achieving lysis for cells or bacteria that are hard to lyse by other means if the cross contamination could be avoided for example by increasing the distances between adjacent spots. Black silicon nanopikes have been shown to perforate bacteria, lysing and killing them.^[14]

The SHB black silicon areas were never observed to perforate cells. The likely reason is the plastron and the very low solid fraction of the surface; when the cells glide on top of these areas, they are barely in contact with the spikes at all (note that the case with the SHL black silicon described above is completely different since there is no protecting air pocket). Remarkably, practically no cells were observed to stick to the superhydrophobic areas throughout all the experiments performed. This is a major benefit since it means that a separate washing step to remove the cells outside the array positions is not needed. Due to these reasons, black silicon SHB surface and planar SHL spots were chosen as the materials for the SHB/SHL arrays for single cell trapping experiments.

One noteworthy issue is that in this work, the focus was on developing a single cell trapping method for subsequent analysis of cell content, so there was no effort to control for evaporation (which was rapid and happened in less than few seconds). However, for applications requiring live cells for culturing, such as drug screening, the drying would need to be eliminated by, for example, humidity control or a protective oil layer. The protective oil layer strategy consists of submerging the SHB/SHL patterned substrate into an oil prior to dragging with the mother droplet. This strategy was confirmed to work in a preliminary experiment for trapping single beads but was not explored further.

The single cell trapping capability of the planar SHL spots was evaluated by two cell types, primary PBMCs obtained from adult blood and immortalized THP-1 cancer cell-line. PBMCs are a group of small mononuclear blood leukocytes of various types (lymphocytes, monocytes, and natural killer cells), typically 10–15 μm in diameter and THP-1 cells are immortalized monocytes and are larger in size. Monocytes are part of the human innate immune system and enriched with cell surface molecules that enable cell migration through the blood vessels to the tissue where they can phagocyte the pathogens. The lymphocyte surface molecules are specialized for antigen recognition and less specialized for cell adhesion and migration.

The results of the effects of cell type, the seeding droplet velocity, and the cell concentration in the suspension are summarized in **Figure 3**. In terms of single-cell capture efficiency, the highest mean single-cell occupancy rate (SOR) 36.0% was achieved with low-concentration PBMC suspension and 10 mm min⁻¹ seeding velocity (Figure 3a). The velocity of the seeding droplet had a clear effect on the SOR PBMCs. Increasing the velocity from 10 to 90 mm min⁻¹ led to a decrease in mean SOR from 36.0% to 20.5%. Interestingly, the velocity effect was not observed with THP-1 (Figure 3a). The different response on the seeding velocity may be explained by the differing surface chemistry and adhesion properties between the cell types and highlights the differences between cell-types.

The cell suspension concentration displayed the same effect for both cell types on the mean SOR. Counter-intuitively, lower concentration led to higher mean SOR (Figure 3b,d). Reducing the cell concentration from 20 000 cells per μl (Figure 3c) to 10 000 cells per μl (Figure 3b) yielded roughly twice as high mean SOR (Figure 3a). This effect could be attributed to finite diameter of the capillary channel between the mother droplet and the hydrophilic region, which likely works as a pathway for the cell to migrate into the hydrophilic spot; we suggest that the capillary channel is more likely to be clogged when the cell suspension concentration is increased, hindering the cell migration to the spot.

Overall, the mean SOR is higher at lower seeding velocities and is independent of the cell type. The ratio of trapped multiple cells to single cells was lower than suggested by Poisson distribution, that is, the proportion of trapped multiple cells was significantly lower than expected (Table S1, Supporting Information). This shows that the single cell trapping is based on the size of the spots that matches roughly twice the diameter of the cells, like was shown for the polystyrene beads even though cells are more heterogenous in size, shape, and malleability. The only exception to this was PBMC cells which tended to deposit as groups into the spots at higher rates using low seeding velocity and low cell concentration (Table S1, Supporting Information).

3. Conclusion

In conclusion, we have shown how SHB/SHL microarray with spot sizes in the same range as cells can be used for single cell trapping based on size exclusivity instead of Poisson statistics. The obtained optimized single cell trapping rate for both cell types was around 30%, which is higher than what is possible by dilution and Poisson distribution. A major advantage is that this level of trapping was obtained by a very simple single step process consisting only of dragging a cell suspension droplet along the surface without any cleaning steps needed. The effects of the spot type, the cell type, the cell concentration, and the velocity of the cell suspension droplets were studied and shown to all have an effect on the trapping process and the obtained cell deposition distribution. The 28 000 spots per cm^2 with 30% capture efficiency means that 10 000s of single cells can be captured (with a rate of several 1000s of cells deposited per minute). This number of cells is on par with or outperforms state-of-the-art commercial single cell platforms such as 10x Genomics Chromium droplet system. Further development for single cell sequencing applications would need linking of the cell DNA or RNA with synthetic spot specific barcoding oligonucleotides. This novel cell capture concept shows potential to various novel high throughput single cell applications.

4. Experimental Section

Superhydrophobic/Superhydrophilic Array Fabrication: The arrays with black silicon SHL spots were fabricated by first etching the black silicon by a maskless cryogenic DRIE black silicon process (Sainiemi). The process parameters (Oxford Plasmalab System 100 ICP-DRIE) were $-110\text{ }^\circ\text{C}$ temperature, 10 mTorr pressure, ICP power 1000W, forward power 6W, and the gas flows were 18 sccm for O_2 and 30 sccm for SF_6 , respectively. The wafer was then covered with a hydrophobic coating using a PECVD process (Oxford Plasmalab 80). The process parameters were 250 mTorr pressure, 50W power, and 100 sccm CHF_3 flow. Next, the hydrophilic areas were defined by optical lithography using AZ 4562 photoresist (spin coated 4000 rpm for 30s), exposed for 10s (Süss MicroTec MA-6 with 365 nm wavelength), and developed for 10 min in AZ 351B. The fluoropolymer was then removed from areas not protected by resist using oxygen plasma reactive ion etching (Oxford Plasmalab 80). The parameters were 250 mTorr pressure, 50 W power, 45 sccm O_2 , and 5 sccm Ar. The photoresist was then removed by ultrasonically in acetone leaving the fluoropolymer intact. To fabricate the arrays with planar SHL spots, first PECVD oxide was deposited on a silicon wafer (Oxford Plasmalab 80). The parameters were 1000 mTorr pressure,

20 W power, $300\text{ }^\circ\text{C}$ temperature, 8.5 sccm SiH_4 flow, 7 10 sccm N_2O flow, and 161.5 sccm N_2 flow. The oxide was patterned by optical lithography (AZ 5214E resist, 4000 rpm 30 s spincoating, 2.5 s exposure) and reactive ion etching of the oxide (200 mTorr pressure, 30 W power, 25 sccm CHF_3 , and 25 sccm Ar). After this, the process was identical to the black silicon SHL spot arrays (the oxide acts as an etch mask for the black silicon process).

Wettability Characterization: The advancing and receding water contact angles were measured with the sessile droplet needle method using contact angle goniometer (THETA, Biolin Scientific). The advancing contact angle was measured from 1 to 4 μl and the receding contact angles were measured from 4 to 1 μl . The pumping rate was $0.1\text{ }\mu\text{l s}^{-1}$. For very low angles ($<5^\circ$), quantitative measurement was not possible.

Cell Suspension: The experiments were conducted using two different cell populations: peripheral blood mononuclear cells (PBMCs) and THP-1 immortalized cancer cells. PBMCs are primary cells isolated from adult volunteers' blood samples (Ethical committee decisions 103/13/03/01/2016 and 147/13/03/01/16, Hospital district of Helsinki and Uusimaa). PBMCs consist of small blood mononuclear white blood cells (10–15 μm in diameter) such as lymphocytes, NK-cells, and monocytes. On the contrary, THP-1 cancer cell-line (monocytes) originates from human leukemia patients and is larger in size compared to PBMCs (20 μm in diameter).

PBMCs were isolated from EDTA blood using Ficoll Leukosep tubes. Cells were cultured in RPMI-1640 medium (Lonza) overnight before the experiment. THP-1 (non-adherent) cancer cell-line was grown in RPMI-1640 medium (with Glutamax + Penicillin-Streptomycin + FCS + HEPES, all from ThermoFisher). Both cell types were stained using Cell tracker TM Blue CMAC (working concentration of 25 μM , Invitrogen). They were washed with solution of PBS and 0.01% BSA (Bovogen) and diluted to working concentration of 100 000 or 200 000 cells in 10 μl PBS/BSA.

Bead and Cell Deposition: The beads and cells were deposited using micro pipette (static) and a moving platform (dynamic), both digitally controlled. The pipette (z-axis) was orthogonal to the platform (x-axis and y-axis). The hydrophilic spot array was first placed and aligned onto the platform. Next, a 10 μl bead/cell suspension droplet was formed, but not released, on the pipette tip and brought to contact with the array by moving the pipette holder (z-axis). After contact, the platform was set to move along the x-axis with controlled velocity, 10 to 100 mm min^{-1} , for distance of 5 mm. After the platform had travelled the 5 mm distance, the deposition was completed.

Bead and Cell Deposition Analysis: The deposited beads were imaged using optical microscope and the image analysis was conducted by tabulating the number of beads on each spot (spot occupancy). The cells were imaged using EVOS light microscopy with DAPI light cube (Plan Fluor, NA 0.30, dry) and Scanning electron microscope (SEM) pictures were taken using SEM EBL Zeiss Supra 40 microscope (EHT: 3.00 kV, WD 4.9–5.6 mm, Signal A: InLens). Image analysis was conducted with imageJ software and by tabulating the number of cells deposited on each spot (cell occupancy). The mean occupancy rate and standard deviation was calculated using three to five different images for each deposition run with differing seeding velocity, spot size, cell concentration, cell type, and bead type.

Supporting Information

Supporting Information is available from the Wiley Online Library or from the author.

Acknowledgements

P.R. and P.E. contributed equally to this work. Funding from the Academy of Finland (#297360) and Business Finland (#1906/31/2016 and #6681/31/2016) is acknowledged.

Conflict of Interest

The authors declare no conflict of interest.

Data Availability Statement

Research data are not shared.

Keywords

biomaterials, black silicon, cell-repellent, droplet, microwell, nanopillars, single cell analysis, wettability patterning

Received: January 28, 2021

Revised: February 17, 2021

Published online: March 7, 2021

-
- [1] A. Lafuma, D. Quéré, *Nat. Mater.* **2003**, *2*, 457.
[2] A. B. D. Cassie, S. Baxter, *Trans. Faraday Soc.* **1944**, *40*, 546.
[3] A. Tuteja, W. Choi, M. Ma, J. M. Mabry, S. A. Mazzella, G. C. Rutledge, G. H. McKinley, R. E. Cohen, *Science* **2007**, *318*, 1618.
[4] T. L. Liu, C.-J. C. Kim, *Science* **2014**, *346*, 1096.
[5] V. Rontu, V. Jokinen, S. Franssila, *J. Microelectromech. Syst.* **2020**, *29*, 54.
[6] V. Jokinen, L. Sainiemi, S. Franssila, *Adv. Mater.* **2008**, *20*, 3453.
[7] E. Ueda, P. A. Levkin, *Adv. Mater.* **2013**, *25*, 1234.
[8] F. L. Geyer, E. Ueda, U. Liebel, N. Grau, P. A. Levkin, *Angew. Chem., Int. Ed.* **2011**, *50*, 8424.
[9] V. Jokinen, R. Kostianen, T. Sikanen, *Adv. Mater.* **2012**, *24*, 6240.
[10] M. J. Hancock, F. Yanagawa, Y.-H. Jang, J. He, N. N. Kachouie, H. Kaji, A. Khademhosseini, *Small* **2012**, *8*, 393.
[11] Y. Wang, C. E. Sims, P. Marc, M. Bachman, G. P. Li, N. L. Allbritton, *Langmuir* **2006**, *22*, 8257.
[12] V. Jokinen, E. Kankuri, S. Hoshian, S. Franssila, R. H. A. Ras, *Adv. Mater.* **2018**, *30*, 1705104.
[13] S. Movafaghi, V. Leszczak, W. Wang, J. A. Sorkin, L. P. Dasi, K. C. Popat, A. K. Kota, *Adv. Healthcare Mater.* **2017**, *6*, 1600717.
[14] E. P. Ivanova, J. Hasan, H. K. Webb, G. Gervinskas, S. Juodkazis, V. K. Truong, A. H. F. Wu, R. N. Lamb, V. A. Baulin, G. S. Watson, J. A. Watson, D. E. Mainwaring, R. J. Crawford, *Nat. Commun.* **2013**, *4*, 2838.
[15] G. B. Hwang, K. Page, A. Patir, S. P. Nair, E. Allan, I. P. Parkin, *ACS Nano* **2018**, *12*, 6050.
[16] T. Ishizaki, N. Saito, O. Takai, *Langmuir* **2010**, *26*, 8147.
[17] G. Piret, E. Galopin, Y. Coffinier, R. Boukherroub, D. Legrand, C. Slomianny, *Soft Matter* **2011**, *7*, 8642.
[18] P. Bheda, R. Schneider, *Trends Cell Biol.* **2014**, *24*, 712.
[19] E. Z. Macosko, A. Basu, R. Satija, J. Nemes, K. Shekhar, M. Goldman, I. Tirosh, A. R. Bialas, N. Kamitaki, E. M. Martersteck, J. J. Trombetta, D. A. Weitz, J. R. Sanes, A. K. Shalek, A. Regev, S. A. McCarroll, *Cell* **2015**, *161*, 1202.
[20] T. M. Gierahn, M. H. Wadsworth, T. K. Hughes, B. D. Bryson, A. Butler, R. Satija, S. Fortune, J. C. Love, A. K. Shalek, *Nat. Methods* **2017**, *14*, 395.
[21] L. Du, H. Liu, J. Zhou, *Microsyst. Nanoeng.* **2020**, *6*, 33.
[22] W. Xie, D. Gao, F. Jin, Y. Jiang, H. Liu, *Anal. Chem.* **2015**, *87*, 7052.
[23] G. Jogia, T. Tronser, A. Popova, P. Levkin, *Microarrays* **2016**, *5*, 28.
[24] H. Li, Q. Yang, G. Li, M. Li, S. Wang, Y. Song, *ACS Appl. Mater. Interfaces* **2015**, *7*, 9060.
[25] V. Liimatainen, M. Vuckovac, V. Jokinen, V. Sariola, M. Hokkanen, Q. Zhou, R. H. A. Ras, *Nat. Commun.* **2017**, *8*, 1798.